Uranium isotope fractionation during slab dehydration beneath the Izu arc

Heye Freymuth[1,2,3*], Morten B. Andersen[4], Tim Elliott[2]

[1]Department of Earth Sciences, University of Cambridge, Downing Street, Cambridge, Cambridgeshire, CB2 3EQ, United Kingdom (present address)

[2]School of Earth Sciences, University of Bristol, Wills Memorial Building, Queen's Road, Bristol BS8 1RJ, United Kingdom

[3]School of Earth and Environmental Sciences, The University of Manchester, Williamson Building, Oxford Road, Manchester, M13 9PL, United Kingdom

[4]School of Earth and Ocean Sciences, Cardiff University, Main Building, Park Place, Cardiff, CF10 3AT, United Kingdom

*corresponding author, hf325@cam.ac.uk

Abstract

Fluids released from subducted slabs impart characteristic geochemical signatures on volcanic arc magmas and residual slabs transported into the deeper mantle. Yet, the sources and transport mechanisms of trace elements released from the slab are speculative. We investigate fluids released from subducted slabs from the perspective of $^{238}U/^{235}U$ and radiogenic Pb isotope ratios in lavas from the Izu volcanic arc in the Pacific ocean. Izu arc lavas are fluid-dominated end-member type magmas that allow a close characterization of slab fluids. The Izu arc lavas have low $^{238}U/^{235}U$ ratios compared to the bulk Earth and mid-ocean ridge basalt (MORB). The low $^{238}U/^{235}U$ ($\delta^{238}U$ = -0.46 to -0.33 ‰, where $\delta^{238}U = {}^{238}U/^{235}U_{sample}/ {}^{238}U/^{235}U_{CRM145} -1$) is associated with slab-derived fluids low in Th/U that are added to the magma sources. The radiogenic Pb isotope ratios of the lavas form an array between 'Indian' type MORB and subducting sediments that is inconsistent with fluids derived from the altered mafic oceanic crust (AMOC). We infer that 'fluid-mobile' elements, including U and Pb are mobilized from largely unaltered, deeper sections of the mafic crust by migrating fluids that are derived from the dehydration of underlying serpentinites. Uranium is only fluid-mobile as U^{VI} and needs to be oxidised from predominant U^{IV} in unaltered magmatic rocks in order to be mobilised by fluids. Uranium isotope fractionation of ~ 0.2 ‰ in $\delta^{238}U$ during this process is required to generate the low $^{238}U/^{235}U$ in the fluids. We propose that channelized fluid flow through the metamorphosed sheeted dyke and gabbroic sections of

the mafic crust locally oxidizes and mobilizes U. We suggest that U isotope fractionation occurs within the fluid channels and is related to equilibrium isotope fractionation during the oxidation of U and the incorporation of U^{IV} into secondary phases such as epidote, apatite and zircon that grow within the channels. These phases are predicted to carry isotopically heavy U into the deeper mantle beyond subduction zones. The $\delta^{238}U$ is thus tracing the dehydration process of subducting slabs. Similar observations have been made for other, 'stable isotope' systems in different arcs and subduction-related metamorphic rocks, thus highlighting their potential for studying processes occurring within the slabs during subduction. This information is essential for understanding and the partitioning of elements between subducted slabs and the mantle wedge and constraining the role of subduction zones in global geochemical cycles.

1. Introduction

Subduction zones are the principal sites for exchange of elements between Earth's mantle and continents. Subducted slabs are metamorphosed and dehydrate during subduction. The fluids released ultimately drive elemental fluxes that generate the geochemical signatures of arc magmas. They also modify the elemental and isotopic budget of subducting crust before it is transported into the deeper mantle. Uranium (U) is a key element for studying these processes. It is 'fluid-mobile' in its oxidized state (U^{VI}) and forms the parent nuclides for the U-series decay chains and radiogenic ^{206}Pb and ^{207}Pb isotopes. Understanding its behavior provides insight into geochemical fluxes at arcs and is important for the evolution of long-lived mantle reservoirs.

Uranium is the heaviest naturally occurring element. It is comprised of three radioactive isotopes: ^{238}U ($t_{½}$ = 4.47 x 10^9 y), ^{235}U ($t_{½}$ = 7.04 x 10^8 y), and ^{234}U ($t_{½}$ = 2.45 x 10^5 y). Despite their radioactive nature, the long half-lives of ^{238}U and ^{235}U enable their use as geochemical tracers similar to stable isotope systems, i.e. via the variations in $^{238}U/^{235}U$. Natural variations in $^{238}U/^{235}U$ are dominantly related to isotope exchange reactions occurring during oxidation or reduction of U. The $^{238}U/^{235}U$ ratio has consequently found application in low temperature studies where changes in the redox state of U are common (e.g. Stirling et al., 2007; Weyer et al., 2008). The magnitude and direction of U isotope exchange reactions involving changes in the redox state between U^{IV} and U^{VI} are dominantly controlled by the nuclear field shift effect (Bigeleisen, 1996a; Schauble, 2007). In contrast to more common mass dependent isotope fractionation, which scales with the inverse square of temperature, the nuclear field shift effect scales with the inverse of temperature and thus its influence diminishes slower with increasing temperatures (Bigeleisen, 1996b; Fujii et al., 2006). This makes the potential of U isotope fractionation of particular interest for conditions relevant for subduction zones.

Oceanic crust formed at mid-ocean ridges, and returned into the mantle during subduction, is altered as it cools by percolating seawater after formation. This process results in U addition in the top ~600 m of the mafic oceanic crust (e.g. Alt and Teagle, 2003; Bach et al., 2003; Hart and Staudigel, 1982). We use the term altered mafic oceanic crust

(AMOC) to describe this uppermost section of the oceanic crust. Enrichment in U is also ubiquitous in volcanic arc magmas and it is tempting to link elevated U concentrations in arc lavas to subducted AMOC. Yet, mass balance calculations suggest that only 0-50 % of the oceanic crustal U budget is released from subducted slabs within subduction zones (Elliott et al., 1999; Kelley et al., 2005). The major fraction of subducted U is thus transported beyond subduction zones into the deeper mantle. Recently, Andersen et al. (2015) explored the planetary-scale cycling of U from the perspective of $^{238}U/^{235}U$ ratios. Volcanic arc lavas from the Mariana arc were found to have lower $^{238}U/^{235}U$ ratios than the bulk Earth and mid-ocean ridge basalts (MORB). The $^{238}U/^{235}U$ ratios in the Mariana arc samples correlate with indices of fluid addition (e.g. high Ba/Th, low Ce/Pb and low Th/U, see also Avanzinelli et al., 2012) with the most relatively 'fluid-rich' samples having the lowest $^{238}U/^{235}U$ ratios, suggesting that isotopically light U is added to the sub-arc mantle via slab-derived fluids. However, the ultimate source of the fluid-transported U and the mechanism to generate the light U isotope ratios in the fluids are currently unknown.

Altered mafic oceanic crust (~180 million year old) from ODP Site 801 outboard the Mariana arc was studied by Andersen et al. (2015) to constrain the composition of subducted material. The bulk AMOC sampled across the upper ~400 m at that site has a higher average $^{238}U/^{235}U$ than the bulk Earth and MORB but isotopically light U is present in the top ~110 m. Andersen et al. (2015) thus suggested that preferential sampling of uppermost AMOC altered at dominantly oxidized conditions can lead to release of isotopically light U from subducted slabs. Alternatively, the authors suggested that U isotope fractionation during slab dehydration within subduction zones could cause the fluids to have elevated $^{238}U/^{235}U$ ratios. A slab dehydration model including isotope fractionation has previously been suggested to explain heavy Mo isotope ratios in the Mariana arc lavas (Freymuth et al., 2015). In this model, fluids are released from dehydrating serpentinites underneath the mafic oceanic crust (John et al., 2004; Spandler and Pirard, 2013; Ulmer and Trommsdorff, 1995) and fluid-mobile elements can be sequestered from the entire, several kilometers thick mafic oceanic crust by the upwardly migrating fluids. Derivation of U from the entire crust or just the upper, most altered portion has fundamentally different implications for the mass balance of trace elements in subduction zones, the composition of residual slabs transported into the deeper mantle, and the dehydration mechanism of subducting slabs. It is therefore important to distinguish between these scenarios.

Here we present U isotope data for samples from the Izu volcanic arc. The Izu arc is an oceanic arc in the Western Pacific Ocean with highly depleted trace element signatures when compared to other oceanic arcs. It located at the northern end of the Izu-Bonin-Mariana arc system (Fig. 1) and thus shares many input parameters with the Mariana arc. However, Izu arc lavas notably differ from those erupted in the Marianas by containing a substantially lower fraction of sediment-derived melt components (e.g. (Freymuth et al., 2016b; Stern et al., 2004; Taylor and Nesbitt, 1998). The trace element depleted character and lack of sedimentary overprint in the Izu arc make it a global end-member that allows for a close examination of the compositions of fluids derived from the dehydration of subducting slabs and their associated

trace element budgets. In addition to U isotope ratios, we also present new radiogenic Pb isotope data for the Izu arc lavas. Lead isotope ratios offer the possibility to distinguish between fluids generated from the altered and unaltered subducted MORB and, due to the fluid-mobile attributes of both elements, provide a useful reference for the U isotope ratios.

2. Sample description and analytical methods

Izu arc lava samples are from various islands along the Izu arc: Oshima, Niijima. Miyakejima, Hachijojima, Aogashima, and Torishima. All islands are located at the volcanic front except for Niijima which is in the rear arc between Oshima and Miyakejima (Fig. 1). The samples are basalts and basaltic andesites with the exception of one andesitic sample from Aogashima. Their major and trace element concentrations, radiogenic Sr, Nd, and Hf isotope ratios and U-series data are reported in Freymuth et al. (2016b).

The preparation of rock powders is described in Freymuth et al. (2016b). For Pb isotope analysis approximately 25 mg of powder was dissolved in a HF/HNO_3/HCl mixture followed by complete dissolution of the samples in 6M HCl. The separation of Pb from the rock matrix and Pb isotope analysis was performed as described in Freymuth et al. (2016a). Results for rock standards analysed together with the samples were: JB-2 $^{206}Pb/^{204}Pb$ = 18.343 ± 0.008, $^{207}Pb/^{204}Pb$ = 15.562 ± 0.006, $^{208}Pb/^{204}Pb$ = 38.276 ± 0.023 (n=5) BCR-2: $^{206}Pb/^{204}Pb$ = 18.764 ± 0.016, $^{207}Pb/^{204}Pb$ = 15.627 ± 0.002, $^{208}Pb/^{204}Pb$ = 38.743 ± 0.011 (n=3) (errors are 2σ standard deviations, n = number of analyses), see Table 1. Total analytical blanks were 8-17 pg Pb and negligible compared to the amount of Pb processed for each sample.

For U isotope analyses the ^{233}U-^{236}U double spike IRMM-3636 was added to 0.3-1.0 g of rock powder which was then dissolved in a HF/HNO_3/HCl mixture in 60 ml Savillex beakers followed by dissolution in 6M HCl. The latter step was repeated up to three times until complete dissolution was achieved. For 1 g samples up to 50 ml 6M HCl was added in the final stage. Uranium was separated from the matrix on columns with 1 ml TRU-Spec (50-100 μm). Samples were loaded and matrix was eluted in 22 ml 1M HNO_3 followed by 8 ml 4M HCl and 5ml 0.4M HCl. Uranium was then collected in 7 ml 0.1M HCl+0.3M HF. The samples were then dried and the column repeated to further purify the U fraction. After the second column, the U fraction was dried and a 50:50 mixture of conc. HNO_3 :30 % H_2O_2 was added to oxidise organic material derived from the resin. Samples were then taken up in 0.4M HCl-0.05M HF for analyses on a Thermo Neptune MC-ICPMS at the University of Bristol. Details of the measurement setup and data correction for U measurements are described in Andersen et al. (2015). Results for the BCR-2 standard analysed together with the samples were: $\delta^{238}U$ = -0.288 ± 0.016, ($^{234}U/^{238}U$) = =1.0027 ± 0.0006 (Table 1) in agreement with previous analysis of this standard (Andersen et al. 2015). The $^{238}U/^{235}U$ ratios are reported as $\delta^{238}U$ relative to the CRM 145 standard ($\delta^{238}U = {}^{238}U/^{235}U_{sample}/ {}^{238}U/^{235}U_{standard} -1$) and $^{234}U/^{238}U$ ratios as ($^{234}U/^{238}U$) activity ratios.

3. Results

Uranium and Pb isotope ratios for Izu arc lavas are reported in Table 1. Uranium isotope ratios in the Izu arc lavas ($\delta^{238}U$ = -0.333±0.019 to -0.476±0.017) mostly overlap with previously reported data from the Mariana arc (Fig. 2), but extend to lower values of $\delta^{238}U$ in samples from Oshima and Hachijojima while the rear-arc samples from Niijima have significantly higher $\delta^{238}U$. As for the Mariana arc lavas, there is no trend between $\delta^{238}U$ and indices of differentiation (Fig. 2a). Both Izu and Mariana arc suites have low $\delta^{238}U$ values compared to MORB (Fig. 2b). The Mariana arc lavas form a well-defined positive trend in Th/U vs. $\delta^{238}U$ space (R^2 = 0.87, Fig. 2). Most samples from the Izu islands plot at the depleted, low Th/U end of the Mariana arc array, but with a significant range in $\delta^{238}U$ values. Samples from Torishima plot below the Mariana arc array while Niijima plots along the array with higher Th/U and $\delta^{238}U$ values. Activity ratios of ($^{234}U/^{238}U$) in the Izu arc lavas are either at secular equilibrium or slightly elevated (by up to 3.4 ‰; Table 1). This ratio can be used as a potential indicator for post-eruptive sample alteration or assimilation of a seawater altered volcanic basement because meteoric waters and seawater have substantially elevated ($^{234}U/^{238}U$). We previously used a threshold of ($^{234}U/^{238}U$) < 1.005 to consider sample alteration insignificant as below this ratio genetically related samples do not differ significantly in their U-series systematics (Freymuth et al., 2016b). We therefore consider the U isotope ratios of our samples to represent magmatic values.

Sediment samples from ODP Sites 801 and 802 outboard the Mariana arc were previously analyzed by Andersen et al. (2015). Pelagic clays dominate the budgets of most incompatible elements of interest in the sediment column outboard the Izu arc (Hauff et al., 2003). Two samples of pelagic clays from ODP Site 801 have $\delta^{238}U$ = -0.350 ± 0.013 and $\delta^{238}U$ = -0.358 ± 0.013, respectively, and fall within the range of the Izu and Mariana arcs, albeit at higher Th/U ratios (Fig. 2b). The U isotope ratios of the pelagic clays are similar to those of seawater ($\delta^{238}U \approx$ -0.39) (Andersen et al., 2016; Stirling et al., 2007; Tissot and Dauphas, 2015; Weyer et al., 2008), detrital siliceous sediments (-0.32 ± 0.06; Andersen et al., 2016), and continental and marine sediments (encompassing calcareous sands, siliceous oozes, sandstone, and graywacke; $\delta^{238}U$ = -0.30 ± 0.05) (Tissot and Dauphas, 2015).

Altered mafic oceanic crust sampled at the same ODP Site has lower Th/U ratios compared to the arc lavas but is highly variable in $\delta^{238}U$. Composite samples (powders mixed in representative proportions to the observed lithologies in the drill core) from the upper 0-100 m of the AMOC have light U isotope compositions ($\delta^{238}U$ = -0.436 ± 0.042) (Fig. 2b) whereas sections from 110-220 m and 220-420 m are substantially isotopically heavier ($\delta^{238}U$ = +0.164 ± 0.086 and -0.145 ± 0.045, respectively). The variability in $\delta^{238}U$ within the AMOC was suggested to be related to changes in alteration style with U incorporation under dominantly oxidised conditions in the top of the AMOC and U incorporation under variably reducing conditions in deeper parts (Alt and Teagle, 2003; Andersen et al., 2015; Kelley et al., 2003).

Lead isotope ratios in the Izu arc front lavas fall within the range of previously reported data (Fig. 3). They plot at the radiogenic end of Indian-type MORB at Δ8/4 approximately +40 (with Δ8/4 being the vertical deviation in $^{208}Pb/^{204}Pb$ from the reference best fit line of $^{206}Pb/^{204}Pb$ vs $^{208}Pb/^{204}Pb$ for Northern Hemispheric mantle-derived basalts, (Hart, 1984). They form a linear trend between average Indian MORB and sediment from ODP Site 1149. However, as with U and noted by previous authors (Taylor and Nesbitt, 1998) the Pb isotope ratios in each volcanic front island vary little when compared to the total isotopic variation within the arc (Table 1).

4. Discussion

4.1 Origin of the 'fluid' trace element signature in Izu arc lavas

Previous studies have shown that U and Pb are both mobilized from the slab during subduction, albeit with a higher fraction of Pb released from the slab beneath the volcanic front (Elliott et al., 1999; Kelley et al., 2005). Ratios of Nb/U and Ce/Pb in the Izu arc lavas (Fig. 4) are substantially lower than the canonical values of MORB (Hofmann et al., 1986), suggesting that U and Pb budgets are strongly influenced by additions from the subducted slab. Radiogenic Pb isotope ratios have previously been used as a means to trace fluid transport from the slab to arc magma sources and a dominant contribution from the mafic oceanic crust to the arc magma Pb budget was inferred (Miller et al., 1994). Before discussing the U isotope systematics of the Izu arc lavas, we therefore first examine their radiogenic Pb isotope compositions.

The linear trends of the Izu arc lavas in Pb isotope ratio plots (Fig. 3) have been interpreted as two component mixtures. The radiogenic Pb component is generally thought to represent subducted sediments (Hauff et al., 2003; Hochstaedter et al., 2001; Ishizuka et al., 2003; Straub et al., 2009; Taylor and Nesbitt, 1998; Tollstrup et al., 2010). To explain the 'Indian' Pb isotope character of the unradiogenic Pb end-member, some studies suggest the sub-arc mantle represents this component (Hauff et al., 2003; Hochstaedter et al., 2001; Ishizuka et al., 2003; Kimura et al., 2010; Tollstrup et al., 2010). Yet, as pointed out by Straub et al. (2009) slab-mantle mixtures are inconsistent with the strong enrichment of Pb in the arc lavas relative to similarly incompatible elements. In keeping with the notion that Pb is highly fluid-mobile, Straub et al. (2009) instead suggest that the unradiogenic Pb is derived from a slab derived fluid and relate the high Δ8/4 'Indian' isotopic character of the fluid to the tapping of an 'Indian' mantle reservoir by the now subducted, ~120 Ma crust originally generated at the Izanaghi-Pacific ridge. Importantly, the high Δ8/4 composition of the inferred fluid component does not allow for significant contribution of the low Δ8/4 AMOC to the fluid budget (Fig. 3). The unradiogenic Pb isotope signature of the fluid is therefore not derived from the AMOC.

The low Δ8/4 composition of the AMOC is caused by radiogenic decay of U in the ~120 Ma crust since its addition

during near-ridge alteration of the mafic crust (e.g. Bach et al., 2003; Hart and Staudigel, 1982). Bach et al. (2003) provided a detailed transect through DSDP/ODP Hole 504B of ~6 million years old AMOC in the eastern Pacific ocean which shows substantially elevated, if variable, U/Pb ratios in the upper 800 m. The underlying sheeted dyke complex does not display unusually high U/Pb ratios and will therefore not evolve to elevated $^{206}Pb/^{204}Pb$ and $^{207}Pb/^{204}Pb$ ratios. By inference, the gabbro section below the sheeted dykes should also be unaffected by U enrichment. This is consistent with U concentration data from the deep IODP Hole 1256D into 16 Ma Pacific crust showing U enrichments in the upper 1000 m, but little to no U addition below in the sheeted-dyke and gabbro sections (Neo et al., 2009). Similarly to DSDP/IODP Holes 504B and 1256D, the AMOC at ODP Sites 801 and 1149 outboard the Izu and Mariana arcs are also characterized by high U/Pb, but these sites only penetrate ~470 m and ~133 m into the mafic oceanic crust, respectively, and do not document the transition to lower, MORB-type U/Pb with depth as seen in DSDP/IODP Holes 504B and 1256D. The unradiogenic, high Δ8/4 Pb transported by slab-derived fluids in the Izu arc must originate from deeper stratigraphic levels of the oceanic crust, below ~800 m if DSDP/IODP Holes 504B and 1256D are representative of the subducted crust. For the purpose of this study we refer to this reservoir as middle-lower mafic crust, which approximately corresponds to the metamorphosed sheeted dyke and gabbroic sections originally produced at fast spreading ridges (layers 2b and 3).

The derivation of unradiogenic Pb from the middle-lower mafic crust is consistent with a model in which the fluid is sourced from the dehydration of subducted lithospheric serpentinites (see review in Spandler and Pirard, 2013). Serpentinization of the lithospheric mantle occurs from circulation of crustal scale faults at transform faults and in normal faults in slow spreading ridges and near the trench as the oceanic plate bends into the subduction zone, thus creating deep fractures that may act as fluid pathways (e.g. Cai et al., 2018; Ranero et al., 2003). Transport of the serpentinite-derived fluid into the mantle wedge requires the fluid to flush through the entire mafic crust. Fluid-mobile trace elements can be mobilised by the serpentinite-derived fluids from the middle-lower mafic crust. Temperatures increase strongly towards the top of the subducted slab and can become hot enough for fluid-saturated melting in the metamorphosed AMOC and subducted sediments (Kelemen et al., 2003). Traces of both sediment and AMOC melts were also suggested to be present in arc magmas (Freymuth et al., 2016b; Turner and Langmuir, 2015). We suggest that melts formed near the top of the slab are the origin of the radiogenic Pb end-member in the Izu arc lavas (Fig. 3, 5c), whereas the Pb mobilized by fluids from the middle-lower mafic crust represent the unradiogenic Pb endmember. Fluid release from the slab may occur beneath the arc front but in cold subduction settings such as the Izu arc, serpentinites partially dehydrate at greater depth. Fluid transport and focusing beneath the arc may then occur within seismic low velocity zones parallel to the slab (e.g. Nakajima et al., 2013). Slab-parallel transport of fluids potentially minimizes the impact of subduction zone thermal parameters on the configuration of volcanic arcs (e.g. the position of the volcanic front relative the depth of the subducting plate) but this has not been explored in detail.

Uranium isotope ratios and Th/U ratios in the Izu arc lavas are similar to or lower than those of the nearby Mariana arc (Fig. 2). The variable Th/U in the Mariana arc has been explored in detail before (Avanzinelli et al., 2012; Elliott et al., 1997) and interpreted as a result of mixtures of low Th/U slab-derived fluids and high Th/U melt components. The positive trend shown by the Mariana arc lavas in Fig. 2a thus requires slab-derived fluids to have distinctly low $\delta^{238}U$. The higher $\delta^{238}U$ end-member can be interpreted as a mixture of melts derived from subducted AMOC and sediments (Fig. 2a). At high $\delta^{238}U$ the Marianas trend intersects a mixing line between the average bulk compositions of AMOC and subducted sediments which suggests that the melt end member is a mixture of these two components.

4.2 A quantitative model of fluid and melt components in Izu arc lavas

4.2.1 U isotope ratios

We previously explored the slab components in the Izu arc lavas from the perspective of U-series disequilibria (Freymuth et al., 2016b). The Izu arc lavas have exceptionally high ($^{230}Th/^{232}Th$) (where brackets indicate activity ratios). We interpreted these as a result of the addition of slab melts to the Izu arc magma sources that are dominantly derived from high ($^{230}Th/^{232}Th$) AMOC (50-90 %) with minor contributions (10-50 %) of subducting sediments with lower ($^{230}Th/^{232}Th$). Here we expand our model to incorporate information from $\delta^{238}U$ and radiogenic Pb isotope ratios in order to constrain the origin of U and Pb in the Izu arc lavas.

The Izu arc lavas are on average more depleted in incompatible elements than the Marianas (Fig. 2b, see also review in Stern et al., 2004) and well-defined inter-island geochemical trends such as seen in the Mariana arc are largely absent in the Izu arc (e.g. Taylor and Nesbitt, 1998). A possible explanation for this absence is the generally minor contribution of sediment melts to the Izu arc magma trace element budget when compared to other inter-oceanic arcs such as the Marianas. This gives a weakly defined 'enriched' geochemical end-member and makes the Izu arc magmas more sensitive to variability in other input parameters such as the sediment/AMOC ratio in the slab component (Freymuth et al., 2016b). Single, slab fluid and melt end-members are therefore not readily defined by the Izu arc U isotope ratios (Fig. 5a). As an initial approximation, the model shown in Fig. 5a assumes a common fluid component for the Mariana and Izu arcs (see table 2 for model parameters) which is to first order consistent with the observations.

Within the Izu arc, samples from Niijima constitute the sediment-melt rich end-member with low ($^{230}Th/^{232}Th$) while the high ($^{230}Th/^{232}Th$) in samples from Torishima are more consistent with a higher AMOC contribution (Freymuth et al., 2016b). Yet, there is no consistent trend in ($^{230}Th/^{232}Th$) vs. $\delta^{238}U$ that would support the sediment/AMOC ratios as a general source of U isotope variation (Fig. 5b). A possible reason why the two isotope systems do not correlate is a

variable U isotope composition of the slab-derived fluid. Samples from Hachijojima have the lowest $\delta^{238}U$ among the Izu arc lavas. A constant fluid composition, similar to that indicated for the Mariana arc lavas, would require the slab melt added to the Hachijojima source to be exceptionally sediment-rich (blue dotted line in Fig. 5a). However, such a slab melt component is not indicated by the ($^{230}Th/^{232}Th$) ratios in Hachijojima samples (Fig. 5b), nor has Hachijojima exceptionally radiogenic Sr or unradiogenic Nd isotope ratios (Taylor and Nesbitt, 1998) that would suggest a larger sediment contribution. It is therefore more likely that the fluids added to the different Izu arc magma sources have variable U isotope ratios and that the fluid added to the Hachijojima source has lower $\delta^{238}U$ (see fluid U isotope variation indicated by arrows in Fig. 5a). Due to the proximity of the Izu islands to the fluid end-member (i.e. their low Th/U) a variation in the fluid $\delta^{238}U$ will have more profound effects on the U isotope composition compared to arc lavas that are less dominated by fluids. While this suggests there is some variability in the fluid U isotope compositions within the Izu arc, it should nevertheless be pointed out that overall the fluids added to the Izu arc sources are distinctly isotopically light when compared to MORB (Fig. 5a).

4.2.2. Pb isotope ratios

A quantitative model can also be developed to explain the Pb isotope systematics (Fig. 5c). The Izu islands form positive trends in Pb-Pb isotope ratios plots (Fig. 3). As with U, their Pb isotope ratios can be modeled as mixtures between slab-derived fluids and slab melts. As discussed above, the fluid carries an unaltered Indian MORB Pb signature and is hence modeled as derived from an average Indian MORB source. The slab melts are modeled as mixtures of AMOC and sediments, similar to Fig. 5a. In general, such a model can account for the Pb isotope composition of the Izu arc lavas with the same parameters as used for the U isotope model (table 2). However, despite both slab fluids and slab melts being suggested to contribute to the U and Pb budget of the Izu arc lavas, there is no systematic trend between U and Pb isotope ratios in the Izu arc lavas (Fig. 5d). As noted above for U, fixed end-member components are unable to explain the trace element variation within the Izu arc lavas. This is also the case for Pb. In particular, samples from Mijakejima have the most unradiogenic Pb isotope ratios (Fig. 5c) which would suggest the largest relative contribution of slab-derived fluids (Taylor and Nesbitt, 1998). Yet, an unusually large fluid contribution for Miyakejima is not obvious from other trace element systematics. For instance, Miyakejima lavas are not unusually enriched in fluid mobile elements such as Ba and Pb (Taylor and Nesbitt, 1998) and the U excess in Miyakejima samples is unremarkable when compared to other Izu islands (Freymuth et al., 2016b). In addition, samples from Oshima and Aogashima show nearly identical Pb isotope compositions (Fig. 5c), yet, these islands have contrasting compositions in other tracers for fluid enrichment. Aogashima is least Ba enriched and shows the lowest U excess while Oshima is most Ba enriched and has the highest U excess among the arc front lavas (e.g. Taylor and Nesbitt, 1998, Freymuth et al. 2016b). These observations suggest that the relatively subtle variations in Pb isotope

ratios in the Izu arc lavas do not directly reflect the relative fluid and melt fractions in their sources.

One possible solution to the discrepancy between the Pb isotope compositions of individual Izu islands and their trace element signatures is that the Pb isotope ratios of the slab-derived fluids also vary within the arc, as suggested by Taylor and Nesbitt (1998). When applied to our model this would require the fluid added to the Miyakejima magma source to have less radiogenic Pb compared to the other islands. Such a scenario would indicate a pre-existing Pb isotope heterogeneity in the mafic oceanic crust subducted at the Izu arc with a less radiogenic source beneath Miyakejima.

Alternatively, the Pb isotope composition of the slab melt added to individual island sources might be variable. While U is approximately equally abundant in sediment and AMOC subducting at the Izu arc, the sediments dominantly control the budget of Pb in the melt component. Sediment-AMOC mixtures therefore plot close to the sediment end-member in Pb isotope space (Fig. 5c). The sediments subducted at ODP Site 1149 also vary significantly in their Pb isotope composition (Fig. 5c). An average of the different sediment units can constitute a suitable end-member for most Izu islands. Yet, any variation in the relative contribution of individual sediment units will have a significant effect on the composition of sediment melts. As such, a more dominant role of sediment unit 4 (radiolarian chert and radiolarian nannofossil chalk and marl) could explain the relatively unradiogenic Pb isotope composition of Miyakejima while the contrasting fluid enrichment based on Pb isotopes vs. other tracers (e.g Ba) could be resolved by invoking a variable contribution of sediment units 1 and 2 (carbonate-free clays and brown pelagic clays).

Changes in relative contributions of individual sediment units should be less noticeable in other isotope systems. Uranium isotope data for marine sediments are currently sparse but with the exception of organic-rich shales and Mn crusts they are similar to seawater within a narrow range of about 0.1 ‰ in $\delta^{238}U$ (Andersen et al., 2016, 2015; Stirling et al., 2007; Tissot and Dauphas, 2015; Weyer et al., 2008), suggesting limited U isotopic variability in the subducted sediment sequence. Among the commonly analyzed radiogenic isotope systems, Nd and Hf in the Izu arc lavas are dominantly derived from mantle material and therefore less sensitive to compositional variations in the sediment melt (Freymuth et al., 2016b; Kimura et al., 2010; Tollstrup et al., 2010) while the highly radiogenic Sr isotope ratios in the subducting sediments when compared to the Izu arc lavas (Plank et al., 2007) indicate a limited influence of subducting sediments on the latter.

4.3 Fractionation of U isotopes during slab dehydration, and consequences for deep recycling of U

We have argued for slab-derived fluids with low $\delta^{238}U$ relative to MORB added to the sources of Mariana and Izu arc lavas (Fig. 5a). Here we address the origin of this distinctive signature. As previously discussed (Andersen et al., 2015),

the preferential sampling of uppermost part of the AMOC could be a source of isotopically light U in the arc magmas (Fig. 2b). However, such a process is inconsistent with the relatively unradiogenic Pb in the same arc lavas (Fig. 3). Instead, we suggest that, similarly to the unradiogenic Pb component, the isotopically light U is ultimately derived from middle-lower mafic crust.

No significant U enrichment has been found in the oceanic crust below 800 m depth (Bach et al., 2003), suggesting that high-temperature alteration has limited effect on the U budget of the middle-lower stratigraphic levels of oceanic crust. Uranium isotope ratios in the middle-lower mafic crust should thus be similar to unaltered MORB with $\delta^{238}U \sim -0.27$ (Andersen et al., 2015). The isotopically light U fluid component in the Izu and Mariana arcs with $\delta^{238}U \sim -0.5$ (Fig. 5a) therefore requires U isotope fractionation during the mobilisation of U via fluids.

Uranium is largely immobile in aqueous when present as reduced (4+) species but efficiently mobilised by aqueous fluids in oxidised (6+) form where it is commonly present as the uranyl ion (UO_2^{2+}) but also forms complexes with fluoride, phosphate, carbonate and sulfate (Langmuir, 1978). In the magmatic environment U is dominantly present as U^{4+} (Wood et al., 1999). Oxidation of U is required for it to become fluid-mobile in the middle-lower mafic crust. Fluids released from serpentinites during antigorite breakdown are oxidized with a suggested presence of SO_4^{2-} or CO_3^{2-} species (Debret et al., 2016; Evans and Tomkins, 2011; Kelley and Cottrell, 2009; Pons et al., 2016). These fluids therefore have the potential to oxidize U in the middle-lower mafic crust. Experimental studies and observations mainly from low-temperature systems suggest that compounds with reduced U are associated with high $\delta^{238}U$ (e.g. Shimokaua and Kobayashi, 1970; Stirling et al., 2007; Wang et al., 2015; Weyer et al., 2008).

Uranium isotope exchange reactions are dominantly controlled by the nuclear field shift effect which causes larger U isotope fractionations compared to mass-dependent effects and fractionates the $^{238}U/^{235}U$ ratio in the opposite sense (Bigeleisen, 1996b, 1996a; Fujii et al., 2006; Schauble, 2007). It is reasonable to assume that isotope exchange reactions during oxidation and mobilization of U from the middle-lower oceanic crust at sub-arc depths will follow the same principles and cause the fluid to have lower $\delta^{238}U$ than the host rock. Uranium oxidation and mobilization from the slab, as also suggested by the U excess commonly observed in arc lavas, thus provides a mechanism to explain the offset in $\delta^{238}U$ between a middle-lower mafic crust with MORB-like $\delta^{238}U = -0.268 \pm 0.036$ (Andersen et al., 2015) and the isotopically light fluid component in the Izu and Mariana arc lavas (Fig. 5a).

The isotopic difference between unaltered MORB and the fluid suggested for the Mariana and Izu arcs requires U isotope fractionation of approximately -0.2 ‰ (Fig. 5a). This is lower than the theoretical equilibrium fractionation between ^{238}U and ^{235}U associated with the oxidation of U (e.g. -0.95 to -0.62 ‰ corresponding to fractionation factors $\alpha = 0.99905$ to 0.9994 at temperatures between 300°C and 700°C, respectively, based on Fuji et al., 2006). Processes that could generate the observed U fractionation during fluid release from the slab are discussed below.

Experimental data by Wang et al. (2015) on the U isotope fractionation during oxidation of dissolved uraninite (U^{IV})

showed lower than the theoretically expected U isotope fractionation. This was likely associated with the adsorption of a fraction of U^{IV} to U^{VI} solid surfaces. Mass balance effects during equilibrium isotope fractionation might further limit U isotope fractionation in the experiments because the solution only interacts with the outer layer of the uraninite (Wang et al. 2015). It is unclear whether these experiments, using pure uranium oxides and short timescales, are applicable to the mobilisation of U from subducted slabs, but they provide potential mechanisms for limiting the $^{238}U/^{235}U$ fractionation.

Alternatively, if assuming open-system rather than closed-system equilibrium, the fluid $\delta^{238}U$ increases with increased amount of U removed from the middle-lower mafic crust. In a Rayleigh distillation model, at least 80 % of the U budget needs to be removed from the mafic crust source to reproduce the Izu arc lava U isotope compositions (assuming an integrated fluid, Fig. 6). Rayleigh models assume a homogeneous residual reservoir. During U mobilization from the middle-lower mafic crust, they reflect local conditions of sections of the crust that are in direct contact with the fluid. Studies of eclogite facies metamorphic rocks suggest that serpentinite-derived fluids pass through the mafic oceanic crust in channels (John et al., 2012, 2004; Rubatto and Hermann, 2003; Spandler et al., 2011; Spandler and Pirard, 2013). Uranium mobilization within the channels is likely very high and should thus be associated with minimal U isotope fractionation (Fig. 6) but fluid-mobile elements are also mobilised to a lower degree in metasomatic halos surrounding the veins on approximately meter length scales (John et al., 2012). The resulting U isotope composition of the fluid is therefore likely to be a mixture of highly isotopically fractionated U from the halos (with high fractions of U remaining, Fig. 6) and less fractionated U from the veins.

Additional U isotope fractionation might occur during incorporation of U into secondary phases during slab metasomatism. Veins resulting from channelised fluid flow contain U-bearing phases such as epidote (allanite), apatite, and zircon (John et al., 2004; Rubatto and Hermann, 2003; Spandler et al., 2011). Their presence can also explain the lower fraction of U mobilization from the slab compared to Pb (Elliott et al., 1999; Kelley et al., 2005). Uranium in these phases is present partly or entirely in its reduced oxidation state (Ervanne, 2004; Finch and Murakami, 1999) while U transported in fluids is present as U^{6+}. Formation of secondary U bearing phases during slab metasomatism thus requires the reduction of U which could be associated with concomitant local oxidation of iron, sulfur or carbon, analogous to the process proposed for ground water (Langmuir, 1978). Reduction of U is associated with an increase in $\delta^{238}U$ and conversely should leave the residual fluid with lower $\delta^{238}U$. In addition, zircons from a variety of localities and ages were found to have high $\delta^{238}U$ compared to their host rocks which has been attributed to a different coordination environment of U in the zircons and host magmas (Hiess et al., 2012). While the mechanism of U incorporation into secondary phases remains to be explored in detail, this process could provide an additional pathway of producing a fluid with low $\delta^{238}U$ compared to the host rock. While currently speculative, this model could be tested by measuring the U isotope composition of vein-hosted secondary phases.

Regardless of whether U isotope fractionation is related to the oxidation of U during mobilization via fluids and/or caused by U incorporation into secondary phases, both models suggest that the fractionation occurs during the channelized fluid migration through the middle-lower mafic crust. Isotope fractionation during fluid release from subducted slabs has also been proposed for stable isotope systems such as Fe (Debret et al., 2016; Inglis et al., 2017; Williams et al., 2018), Zn (Pons et al., 2016), and Mo (Freymuth et al., 2015). While additional examples exist where stable isotope compositions appear to be related to source inputs (El Korh et al., 2017; Nielsen et al., 2016), this suggests that stable isotope fractionation within slabs is common during subduction. It also highlights the use of stable isotope systems as tracers for processes acting within the subducted slabs and contrasts these with the more commonly used radiogenic isotope systems that exclusively trace input components.

Variable fluid/rock ratios are thought to substantially affect the element transport during channelized fluid flow (John et al. 2004). Such variations may also explain the minor variation in the fluid U isotope compositions suggested for the different Izu arc islands (Fig. 5a). Higher fluid/rock ratios should lead to decreased fractions of U remaining in the slab and thus decrease the $\delta^{238}U$ of the fluids (Fig. 6). These would indicate local heterogeneity beneath the Izu islands that cause the fluids to migrate through variably shaped networks of channels. The change in overall slab geometry with an increasing subduction angle from north to south (Stern et al., 2004), however, does not appear to affect the U isotope composition of the arc magmas as these are uncorrelated to the along-arc location of the Izu islands.

5. Conclusions

Volcanic arc magmas have long been known to be enriched in 'fluid-mobile' elements that are thought to be derived from subducted slabs. Yet, how and where in the slabs these elements are mobilized is often unconstrained. Magmas produced in the Izu arc have trace element compositions that are dominated by fluid addition and are therefore ideally suited to study this process. Isotopically distinct U and Pb are present in the Izu magma sources. Our data suggest that slab-fluids are associated with low $\delta^{238}U$ and unradiogenic Pb isotope ratios. The data support a model in which the fluids are externally derived from lithospheric serpentinites and flush through the mafic oceanic crust where they acquire their budget of fluid-mobile elements before reaching upper levels of the slab where temperatures are sufficient to cause fluid-saturated melting of AMOC and subducted sediments. This melt has higher $\delta^{238}U$ and more radiogenic Pb isotope ratios. On an intra-arc scale within the Izu arc, there is no correlation between the U and Pb isotope ratios and other tracers for slab additions, suggesting heterogeneity in U and Pb isotope ratios imparted by compositional variations in the slab components.

Uranium needs to be oxidized in order to be mobilized in significant quantities by hydrous fluids. Serpentinite-derived fluids have previously been suggested to be oxidizing, potentially related to the transport of oxidized species such as

SO_4^{2-} or CO_3^{2-}. Uranium isotope fractionation of about -0.2 ‰ in $\delta^{238}U$ is associated with the oxidation and mobilization of U from the mafic oceanic crust via fluids.

Uranium isotope fractionation can be modeled as an equilibrium isotope exchange reaction between oxidized and reduced U in the mafic oceanic crust but requires large (>50 %) fractions of U to be mobilized as U^{6+}. We suggest that this occurs during channelized fluid flow through largely unaltered, middle-lower mafic crust. Incorporation of U into phases formed during slab metasomatism within the channels such as epidote, apatite, and zircon potentially causes further U isotope fractionation and retains a fraction of U within the slab, thus explaining the smaller fraction of U mobilized from subducted slabs within subduction zones when compared to Pb. These phases are predicted to transport isotopically heavy U into the deeper mantle. As shown for other 'stable' isotope systems, the isotopic composition of U is modified within subduction zones and traces processes of fluid and melt release from subducted plates.

Acknowledgments

HF is funded by a Leverhulme Trust Early Career Fellowship and the Isaac Newton Trust and acknowledges additional funding by grants NE/M000303/1 and NE/L004011/1 from the Natural Environment Research Council (NERC) and a short-term fellowship from the Japan Society for the Promotion of Science. TE acknowledges funding from NERC grants NE/H023933/1 and NE/J009024/1 which funded much of this work. We thank two anonymous reviewers and the editor Tamsin Mather for their time and helpful comments and suggestions. Yoshihiko Tamura, Jun-Ichi Kimura, Osamu Ishizuka, Yoshihisa Kawanabe, Akira Takada, and Kenji Niihori are thanked for sharing their samples from Torishima, Niijima, Hachijojima, Oshima, Aogashima, and Miyakejima, respectively.

References

Alt, J.C., Teagle, D.A.H., 2003. Hydrothermal alteration of upper oceanic crust formed at a fast-spreading ridge: mineral, chemical, and isotopic evidence from ODP Site 801. Chem. Geol. 201, 191–211. http://dx.doi.org/10.1016/S0009-2541(03)00201-8

Andersen, M.B., Elliott, T., Freymuth, H., Sims, K.W.W., Niu, Y., Kelley, K.A., 2015. The terrestrial uranium isotope cycle. Nature 517, 356–359.

Andersen, M.B., Vance, D., Morford, J.L., Bura-Nakić, E., Breitenbach, S.F.M., Och, L., 2016. Closing in on the marine 238U/235U budget. Chem. Geol. 420, 11–22. https://doi.org/10.1016/j.chemgeo.2015.10.041

Avanzinelli, R., Prytulak, J., Skora, S., Heumann, A., Koetsier, G., Elliott, T., 2012. Combined 238U–230Th and 235U–231Pa constraints on the transport of slab-derived material beneath the Mariana Islands. Geochim. Cosmochim. Acta 92, 308–328. https://doi.org/10.1016/j.gca.2012.06.020

Bach, W., Peucker-Ehrenbrink, B., Hart, S.R., Blusztajn, J.S., 2003. Geochemistry of hydrothermally altered oceanic crust: DSDP/ODP Hole 504B – Implications for seawater-crust exchange budgets and Sr- and Pb-isotopic evolution of the mantle. Geochem. Geophys. Geosystems 4, n/a–n/a. https://doi.org/10.1029/2002GC000419

Bigeleisen, J., 1996a. Nuclear Size and Shape Effects in Chemical Reactions. Isotope Chemistry of the Heavy Elements. J. Am. Chem. Soc. 118, 3676–3680. https://doi.org/10.1021/ja954076k

Bigeleisen, J., 1996b. Temperature dependence of the isotope chemistry of the heavy elements. Proc. Natl. Acad. Sci. 93, 9393–9396.

Cai, C., Wiens, D.A., Shen, W., Eimer, M., 2018. Water input into the Mariana subduction zone estimated from ocean-

bottom seismic data. Nature 563, 389. https://doi.org/10.1038/s41586-018-0655-4
Debret, B., Millet, M.-A., Pons, M.-L., Bouilhol, P., Inglis, E., Williams, H., 2016. Isotopic evidence for iron mobility during subduction. Geology 44, 215–218. https://doi.org/10.1130/G37565.1
El Korh, A., Luais, B., Deloule, E., Cividini, D., 2017. Iron isotope fractionation in subduction-related high-pressure metabasites (Ile de Groix, France). Contrib. Mineral. Petrol. 172, 41. https://doi.org/10.1007/s00410-017-1357-x
Elliott, T., Plank, T., Zindler, A., White, W., Bourdon, B., 1997. Element transport from slab to volcanic front at the Mariana arc. J Geophys Res 102, 14991–15019.
Elliott, T., Zindler, A., Bourdon, B., 1999. Exploring the kappa conundrum: the role of recycling in the lead isotope evolution of the mantle. Earth Planet. Sci. Lett. 169, 129–145. http://dx.doi.org/10.1016/S0012-821X(99)00077-1
Ervanne, H., 2004. Oxidation state analyses of uranium with emphasis on chemical speciation in geological media (PhD thesis). University of Helsinki, Helsinki.
Evans, K.-A., Tomkins, A.-G., 2011. The relationship between subduction zone redox budget and arc magma fertility. Earth Planet. Sci. Lett. 308, 401–409. https://doi.org/10.1016/j.epsl.2011.06.009
Finch, R., Murakami, T., 1999. Systematics and paragenesis of uranium minerals. Rev. Mineral. Geochem. 38, 91–179.
Freymuth, H., Elliott, T., Soest, M. van, Skora, S., 2016a. Tracing subducted black shales in the Lesser Antilles arc using molybdenum isotope ratios. Geology 44, 987–990. https://doi.org/10.1130/G38344.1
Freymuth, H., Ivko, B., Gill, J.B., Tamura, Y., Elliott, T., 2016b. Thorium isotope evidence for melting of the mafic oceanic crust beneath the Izu arc. Geochim. Cosmochim. Acta 186, 49–70. https://doi.org/10.1016/j.gca.2016.04.034
Freymuth, H., Vils, F., Willbold, M., Taylor, R.N., Elliott, T., 2015. Molybdenum mobility and isotopic fractionation during subduction at the Mariana arc. Earth Planet. Sci. Lett. 432, 176–186. https://doi.org/10.1016/j.epsl.2015.10.006
Fujii, Y., Hihuchi, N., Haruno, Y., Nomura, M., Suzuki, T., 2006. Temperature Dependence of Isotope Effects in Uranium Chemical Exchange Reactions. J. Nucl. Sci. Technol. 43, 400–406. https://doi.org/10.1080/18811248.2006.9711111

Hart, S.R., 1984. A large-scale isotope anomaly in the Southern Hemisphere mantle. Nature 309, 753–757. https://doi.org/10.1038/309753a0
Hart, S.R., Staudigel, H., 1982. The control of alkalies and uranium in seawater by ocean crust alteration. Earth Planet. Sci. Lett. 58, 202–212. https://doi.org/10.1016/0012-821X(82)90194-7
Hauff, F., Hoernle, K., Schmidt, A., 2003. Sr-Nd-Pb composition of Mesozoic Pacific oceanic crust (Site 1149 and 801, ODP Leg 185): Implications for alteration of ocean crust and the input into the Izu-Bonin-Mariana subduction system. Geochem Geophys Geosyst 4, 8913–.
Hiess, J., Condon, D.J., McLean, N., Noble, S.R., 2012. 238U/235U Systematics in Terrestrial Uranium-Bearing Minerals. Science 335, 1610–1614. https://doi.org/10.1126/science.1215507
Hochstaedter, A., Gill, J., Peters, R., Broughton, P., Holden, P., Taylor, B., 2001. Across-arc geochemical trends in the Izu-Bonin arc: Contributions from the subducting slab. Geochem Geophys Geosyst 2.
Hofmann, A.W., Jochum, K.P., Seufert, M., White, W.M., 1986. Nb and Pb in oceanic basalts: new constraints on mantle evolution. Earth Planet. Sci. Lett. 79, 33–45. https://doi.org/DOI: 10.1016/0012-821X(86)90038-5
Inglis, E.C., Debret, B., Burton, K.W., Millet, M.-A., Pons, M.-L., Dale, C.W., Bouilhol, P., Cooper, M., Nowell, G.M., McCoy-West, A.J., Williams, H.M., 2017. The behavior of iron and zinc stable isotopes accompanying the subduction of mafic oceanic crust: A case study from Western Alpine ophiolites. Geochem. Geophys. Geosystems 18, 2562–2579. https://doi.org/10.1002/2016GC006735
Ishizuka, O., Taylor, R.N., Milton, J.A., Nesbitt, R.W., 2003. Fluid–mantle interaction in an intra-oceanic arc: constraints from high-precision Pb isotopes. Earth Planet. Sci. Lett. 211, 221–236. https://doi.org/10.1016/S0012-821X(03)00201-2
Jenner, F.E., O'Neill, H.St.C., 2012. Analysis of 60 elements in 616 ocean floor basaltic glasses. Geochem Geophys Geosyst 13, Q02005–.
John, T., Gussone, N., Podladchikov, Y.Y., Bebout, G.E., Dohmen, R., Halama, R., Klemd, R., Magna, T., Seitz, H.-M., 2012. Volcanic arcs fed by rapid pulsed fluid flow through subducting slabs. Nat. Geosci. 5, 489–492. https://doi.org/10.1038/ngeo1482
John, T., Scherer, E.E., Haase, K., Schenk, V., 2004. Trace element fractionation during fluid-induced eclogitization in a subducting slab: trace element and Lu–Hf–Sm–Nd isotope systematics. Earth Planet. Sci. Lett. 227, 441–456. https://doi.org/10.1016/j.epsl.2004.09.009
Kelemen, P.B., Rilling, J.L., Parmentier, E.M., Mehl, L., Hacker, B.R., 2003. Thermal structure due to solid-state flow in the mantle wedge beneath arcs, in: Geophys. Monogr. Ser. AGU, Washington, DC, pp. 293–311.
Kelley, K.A., Cottrell, E., 2009. Water and the Oxidation State of Subduction Zone Magmas. Science 325, 605–607.

https://doi.org/10.1126/science.1174156
Kelley, K.A., Plank, T., Farr, L., Ludden, J., Staudigel, H., 2005. Subduction cycling of U, Th, and Pb. Earth Planet. Sci. Lett. 234, 369–383. https://doi.org/10.1016/j.epsl.2005.03.005
Kelley, K.A., Plank, T., Ludden, J., Staudigel, H., 2003. Composition of altered oceanic crust at ODP Sites 801 and 1149. Geochem Geophys Geosyst 4, 8910–.
Kimura, J.-I., Kent, A.J.R., Rowe, M.C., Katakuse, M., Nakano, F., Hacker, B.R., van Keken, P.E., Kawabata, H., Stern, R.J., 2010. Origin of cross-chain geochemical variation in Quaternary lavas from the northern Izu arc: Using a quantitative mass balance approach to identify mantle sources and mantle wedge processes. Geochem Geophys Geosyst 11, Q10011–.
Langmuir, D., 1978. Uranium solution-mineral equilibria at low temperatures with applications to sedimentary ore deposits. Geochim. Cosmochim. Acta 42, 547–569. https://doi.org/10.1016/0016-7037(78)90001-7
Miller, D.M., Goldstein, S.L., Langmuir, C.H., 1994. Cerium/lead and lead isotope ratios in arc magmas and the enrichment of lead in the continents. Nature 368, 514–520.
Nakajima, J., Hada, S., Hayami, E., Uchida, N., Hasegawa, A., Yoshioka, S., Matsuzawa, T., Umino, N., 2013. Seismic attenuation beneath northeastern Japan: Constraints on mantle dynamics and arc magmatism. J. Geophys. Res. Solid Earth n/a–n/a. https://doi.org/10.1002/2013JB010388
Neo, N., Yamazaki, S., Miyashita, S., 2009. Data report: bulk rock compositions of samples from the IODP Expedition 309/312 sample pool, ODP Hole 1256D, in: Teagle, D.A.H., Alt, J.C., Umino, S., Miyashita, S., Banerjee, N.R., Wilson, D.S., and the Expedition 309/312 Scientists, Proc. IODP, 309/312. Integrated Ocean Drilling Program Management International, Inc.
Nielsen, S.G., Yogodzinski, G., Prytulak, J., Plank, T., Kay, S.M., Kay, R.W., Blusztajn, J., Owens, J.D., Auro, M., Kading, T., 2016. Tracking along-arc sediment inputs to the Aleutian arc using thallium isotopes. Geochim. Cosmochim. Acta 181, 217–237. https://doi.org/10.1016/j.gca.2016.03.010
Plank, T., Kelley, K.A., Murray, R.W., Stern, L.Q., 2007. Chemical composition of sediments subducting at the Izu-Bonin trench. Geochem Geophys Geosyst 8, Q04I16–.
Pons, M.-L., Debret, B., Bouilhol, P., Delacour, A., Williams, H., 2016. Zinc isotope evidence for sulfate-rich fluid transfer across subduction zones. Nat. Commun. 7, 13794. https://doi.org/10.1038/ncomms13794
Ranero, C.R., Morgan, J.P., McIntosh, K., Reichert, C., 2003. Bending-related faulting and mantle serpentinization at the Middle America trench. Nature 425, 367–373.
Rubatto, D., Hermann, J., 2003. Zircon formation during fluid circulation in eclogites (Monviso, Western Alps): implications for Zr and Hf budget in subduction zones. Geochim. Cosmochim. Acta 67, 2173–2187. https://doi.org/10.1016/S0016-7037(02)01321-2
Schauble, E.A., 2007. Role of nuclear volume in driving equilibrium stable isotope fractionation of mercury, thallium, and other very heavy elements. Geochim. Cosmochim. Acta 71, 2170–2189. https://doi.org/10.1016/j.gca.2007.02.004
Shimokaua, J., Kobayashi, F., 1970. Separation of Uranium Isotopes by Chemical Exchange. Isot. Isot. Environ. Health Stud. 6, 170–176. https://doi.org/10.1080/10256017008621706
Spandler, C., Pettke, T., Rubatto, D., 2011. Internal and External Fluid Sources for Eclogite-facies Veins in the Monviso Meta-ophiolite, Western Alps: Implications for Fluid Flow in Subduction Zones. J. Petrol. 52, 1207–1236. https://doi.org/10.1093/petrology/egr025
Spandler, C., Pirard, C., 2013. Element recycling from subducting slabs to arc crust: A review. Lithos 170, 208–223. https://doi.org/10.1016/j.lithos.2013.02.016
Stern, R.J., Fouch, M.J., Klemperer, S.L., 2004. An Overview of the Izu-Bonin-Mariana Subduction Factory, in: Eiler, J. (Ed.), Inside the Subduction Factory. American Geophysical Union, pp. 175–222. https://doi.org/10.1029/138GM10
Stirling, C.H., Andersen, M.B., Potter, E.-K., Halliday, A.N., 2007. Low-temperature isotopic fractionation of uranium. Earth Planet. Sci. Lett. 264, 208–225. http://dx.doi.org/10.1016/j.epsl.2007.09.019
Straub, S.M., Goldstein, S.L., Class, C., Schmidt, A., 2009. Mid-ocean-ridge basalt of Indian type in the northwest Pacific Ocean basin. Nat. Geosci 2, 286–289.
Taylor, R.N., Nesbitt, R.W., 1998. Isotopic characteristics of subduction fluids in an intra-oceanic setting, Izu–Bonin Arc, Japan. Earth Planet. Sci. Lett. 164, 79–98. http://dx.doi.org/10.1016/S0012-821X(98)00182-4
Tissot, F.L.H., Dauphas, N., 2015. Uranium isotopic compositions of the crust and ocean: Age corrections, U budget and global extent of modern anoxia. Geochim. Cosmochim. Acta 167, 113–143. https://doi.org/10.1016/j.gca.2015.06.034
Tollstrup, D., Gill, J., Kent, A., Prinkey, D., Williams, R., Tamura, Y., Ishizuka, O., 2010. Across-arc geochemical trends in the Izu-Bonin arc: Contributions from the subducting slab, revisited. Geochem Geophys Geosyst 11, Q01X10–.
Turner, S.J., Langmuir, C.H., 2015. What processes control the chemical compositions of arc front stratovolcanoes? Geochem. Geophys. Geosystems n/a-n/a. https://doi.org/10.1002/2014GC005633
Ulmer, P., Trommsdorff, V., 1995. Serpentine Stability to Mantle Depths and Subduction-Related Magmatism. Science

268, 858–861. https://doi.org/10.1126/science.268.5212.858
Wang, X., Johnson, T.M., Lundstrom, C.C., 2015. Low temperature equilibrium isotope fractionation and isotope exchange kinetics between U(IV) and U(VI). Geochim. Cosmochim. Acta 158, 262–275. https://doi.org/10.1016/j.gca.2015.03.006
Weyer, S., Anbar, A.D., Gerdes, A., Gordon, G.W., Algeo, T.J., Boyle, E.A., 2008. Natural fractionation of 238U/235U. Geochim. Cosmochim. Acta 72, 345–359. https://doi.org/10.1016/j.gca.2007.11.012
Williams, H.M., Prytulak, J., Woodhead, J.D., Kelley, K.A., Brounce, M., Plank, T., 2018. Interplay of crystal fractionation, sulfide saturation and oxygen fugacity on the iron isotope composition of arc lavas: An example from the Marianas. Geochim. Cosmochim. Acta 226, 224–243. https://doi.org/10.1016/j.gca.2018.02.008
Wood, B.J., Blundy, J.D., Robinson, J.A.C., 1999. The role of clinopyroxene in generating U-series disequilibrium during mantle melting. Geochim. Cosmochim. Acta 63, 1613–1620. https://doi.org/10.1016/S0016-7037(98)00302-0

Figures

Figure 1: Map of the Izu Bonin Mariana arc system showing locations of sampled islands in the Izu arc and oceanic drill sites ODP Site 1149 and ODP Site 801. Basemap is from geomapapp (www.geomapapp.org), modified from Freymuth et al. (2016).

Figure 2: Uranium isotope ratios in Izu and Mariana arc lavas, AMOC and marine sediments. a) $\delta^{238}U$ vs. MgO, b) Th/U vs. $\delta^{238}U$. Sediment, AMOC and MORB are average compositions of pelagic sediment, altered mafic oceanic crust, and mid-ocean ridge basalts, respectively. Uranium isotope data for Mariana arc lavas, AMOC and MORB are from Andersen et al. (2015). The sediment is the average of two samples of pelagic clays from ODP Sites 801 outboard the Mariana arc (Andersen et al., 2015). MgO, Th and U concentrations are from Elliott et al. (1997) (Mariana arc) and Freymuth et al. (2016) (Izu arc). The dotted line in b) is a linear regression through the Mariana arc lavas ($R^2 = 0.87$). Error bars represent 2 σ standard errors.

Figure 3: Lead isotope ratios in Izu arc lavas compared to MORB and oceanic sediments. a) $^{208}Pb/^{204}Pb$ vs. $^{206}Pb/^{204}Pb$ b) $^{207}Pb/^{204}Pb$ vs. $^{206}Pb/^{204}Pb$. Large symbols for Izu arc lavas are from this study (Table 1), small symbols are from previously published studies. Indian MORB and Pacific MORB are from PetDB (http://www.earthchem.org/petdb). See supplementary data file for full list of references. The large symbol for Indian MORB is the average of all Indian MORB data. Altered Indian MORB is calculated from the average Indian MORB assuming an age of 130 Ma by first calculating the initial Pb isotope composition at 130 Ma followed by aging for 130 Ma at increased U/Pb and Th/Pb using average U (0.390 ppm), Th (0.173 ppm), and Pb (0.437 ppm) concentrations from altered oceanic crust at ODP Site 801 (Kelley et al., 2003). ODP Site 1149 sediment is the bulk sediment from Plank et al. (2007). NHRL is the northern hemisphere reference line (Hart, 1984).

Figure 4: Ce/Pb vs. Nb/U in Izu and Mariana arc lavas compared to MORB. MORB is the average and standard deviation of data for MORB from Jenner and O'Neill (2012). Symbols are the same as in Fig. 2. Data for Izu arc lavas are from Freymuth et al. (2016).

Figure 5: Uranium and Pb isotope models for Izu arc lavas. a) Th/U vs. $\delta^{238}U$. The Izu and Mariana arc lavas are modeled as mixtures between a slab fluid and a slab melt. The slab fluid represents a hydrous, serpentinite-derived fluid that fluxes through the mafic crust. The slab melt is a mixture of sediment melt and AMOC melt. Markers on mixing lines represent 10 % mixing steps. Model parameters are listed in Table 2 and are the same as in Freymuth et al. (2016) with the following addition: $\delta^{238}U$ of the slab fluid has been chosen based on the trend formed by the Mariana arc lavas (Fig. 2). Sediment melt and AMOC melt U isotope ratios are averages from Andersen et al. (2015). The highlighted range in slab melt compositions from 50-90 % AMOC has previously been suggested for the Izu arc lavas based on their Th isotope ratios (Freymuth et al., 2016b). The blue dotted line indicates mixtures between a slab fluid and a sediment melt as source for Hachijojima lavas (see text for details). b) Th activity ratios vs. $\delta^{238}U$ showing no correlation between the two isotope systems within the Izu arc. Thorium isotope ratios of AMOC and sediment melt (SED) are indicated qualitatively by the arrows. c) $^{208}Pb/^{204}Pb$ vs. $^{206}Pb/^{204}Pb$. The average sediment and individual sediment units from ODP Site 1149 are from Plank et al. (2007). Mixing model parameters are the same as in a). Lead isotope ratios in AMOC are the same as in Fig. 3. d) $^{208}Pb/^{204}Pb$ vs. $\delta^{238}U$.

Figure 6: Rayleigh distillation models for the mobilisation of U from the mafic oceanic crust showing the U isotope composition of a fluid released from the slab and the residual mafic oceanic crust. Also shown is the composition of the integrated fluid assuming that the entire fluid is transported to the arc magma source (labeled 'total fluid'). The initial mafic crust has the composition of MORB ($\delta^{238}U$ = -0.27, Andersen et al. 2015). Three different fractionation models are shown with fractionation factors α = 0.99905, 0.99925 and 0.99940, respectively, representing equilibrium U isotope fractionation for U^{IV} to U^{IV} exchange at temperatures of 300-700°C (Fujii et al., 2006). The grey shaded field indicates the range of U isotope ratios in the Izu arc lavas.

495 Fig. 1

496

497

498

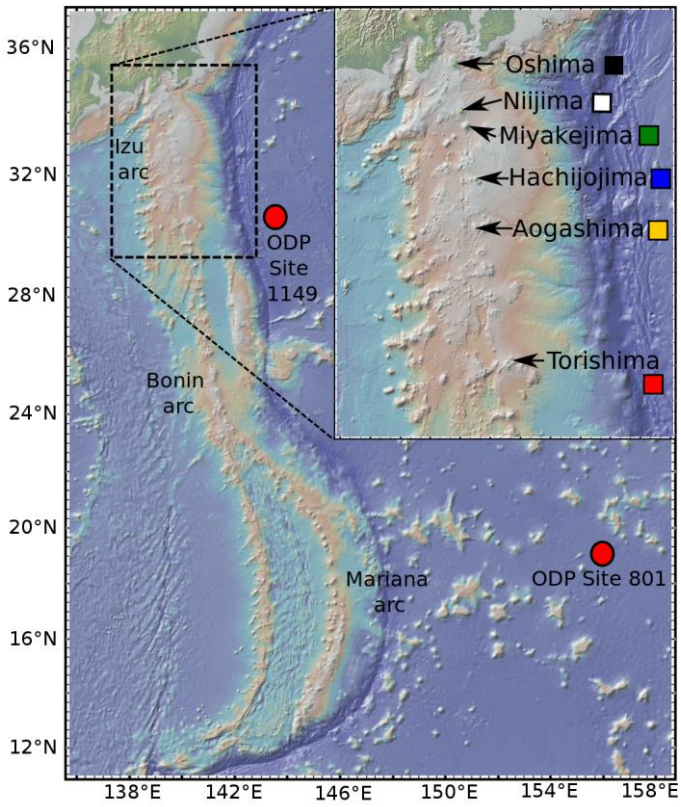

499 Fig. 2

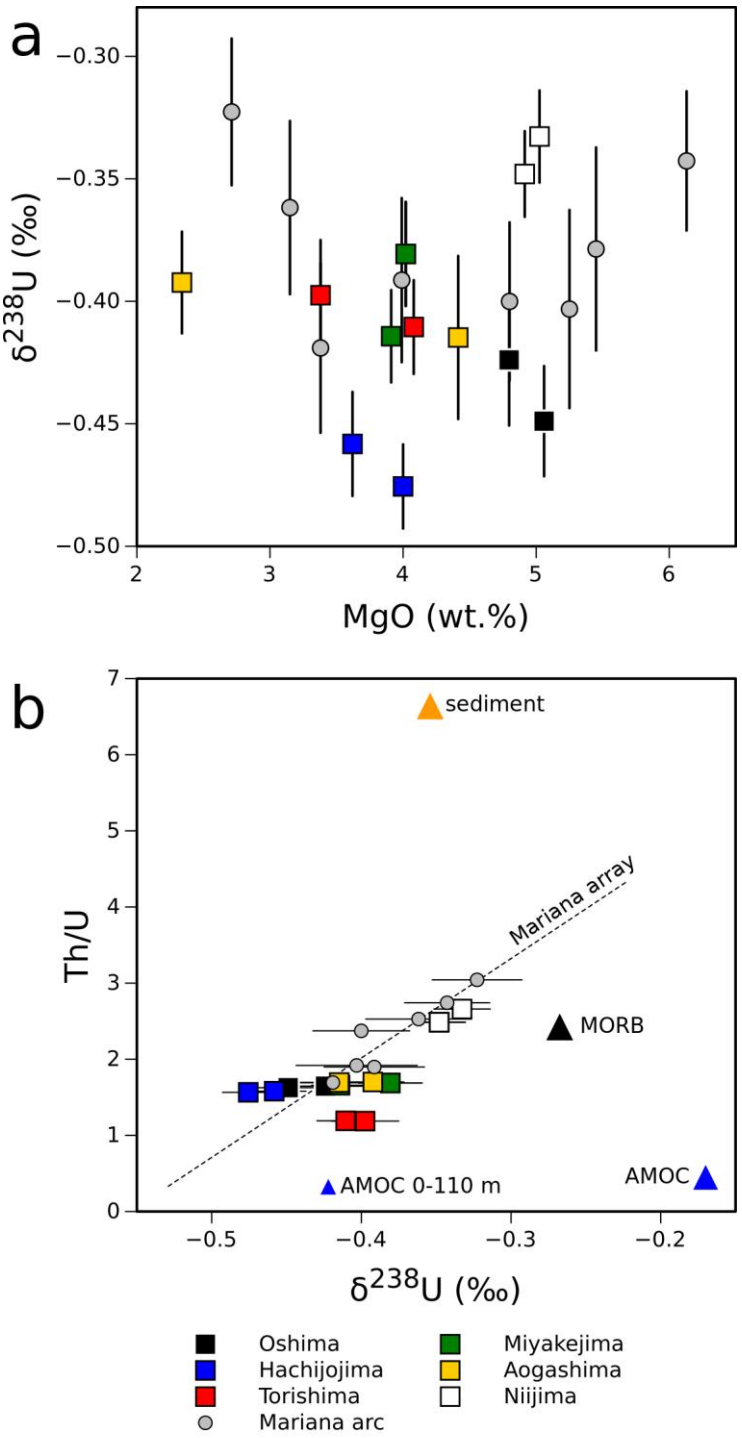
a
−0.30
−0.35
−0.40
−0.45
−0.50
δ238U (‰)
2
3
4
5
6
MgO (wt.%)
b
7
6
5
4
3
2
1
0
Th/U
sediment
Mariana array
MORB
AMOC 0-110 m
AMOC
−0.5
−0.4
−0.3
−0.2
δ238U (‰)
Oshima
Hachijojima
Torishima
Mariana arc
Miyakejima
Aogashima
Niijima

501 Fig. 3

502

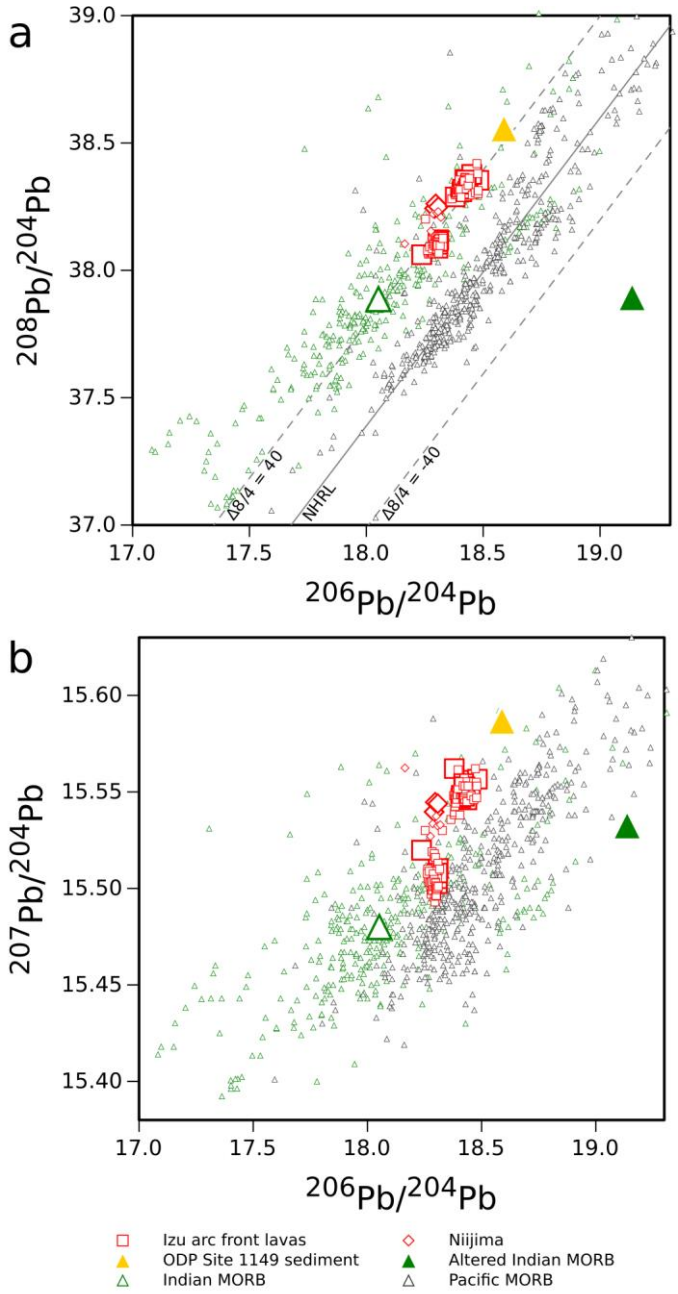
a
39.0
38.5
38.0
37.5
37.0
$^{208}Pb/^{204}Pb$
17.0
17.5
18.0
18.5
19.0
$^{206}Pb/^{204}Pb$
Δ8/4 = 40
NHRL
Δ8/4 = -40
b
15.60
15.55
15.50
15.45
15.40
$^{207}Pb/^{204}Pb$
17.0
17.5
18.0
18.5
19.0
$^{206}Pb/^{204}Pb$
Izu arc front lavas
ODP Site 1149 sediment
Indian MORB
Niijima
Altered Indian MORB
Pacific MORB

503 Fig. 4

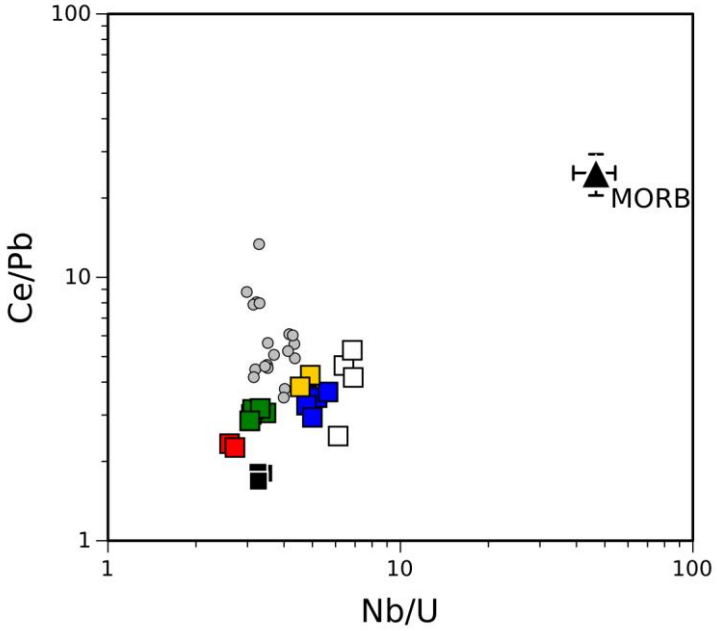

Fig. 5

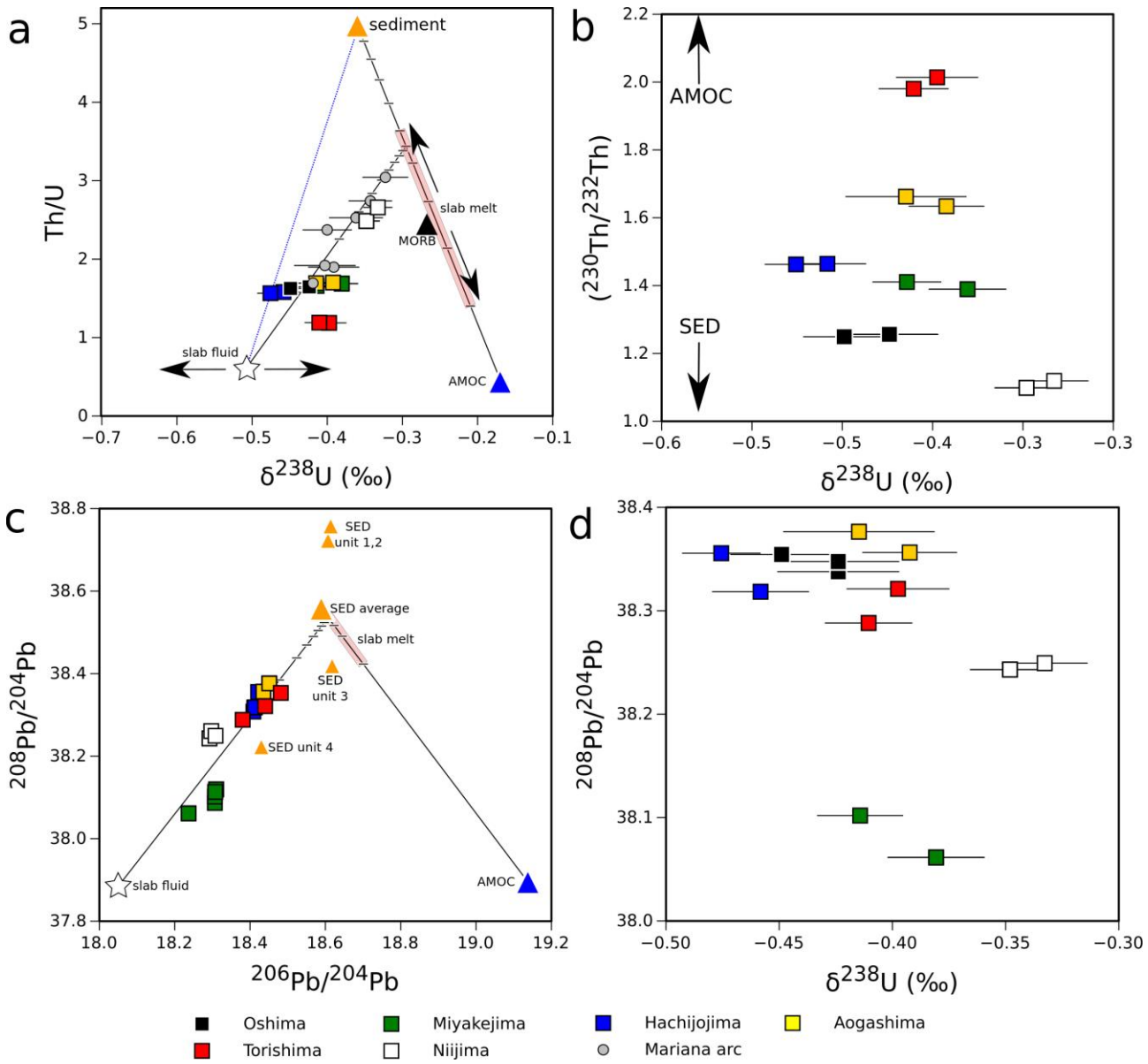
a
sediment
slab melt
MORB
slab fluid
AMOC
Th/U
δ238U (‰)
b
AMOC
SED
(230Th/232Th)
δ238U (‰)
c
SED
unit 1,2
SED average
slab melt
SED
unit 3
SED unit 4
slab fluid
AMOC
208Pb/204Pb
206Pb/204Pb
d
208Pb/204Pb
δ238U (‰)
Oshima
Torishima
Miyakejima
Niijima
Hachijojima
Mariana arc
Aogashima

507 Fig. 6

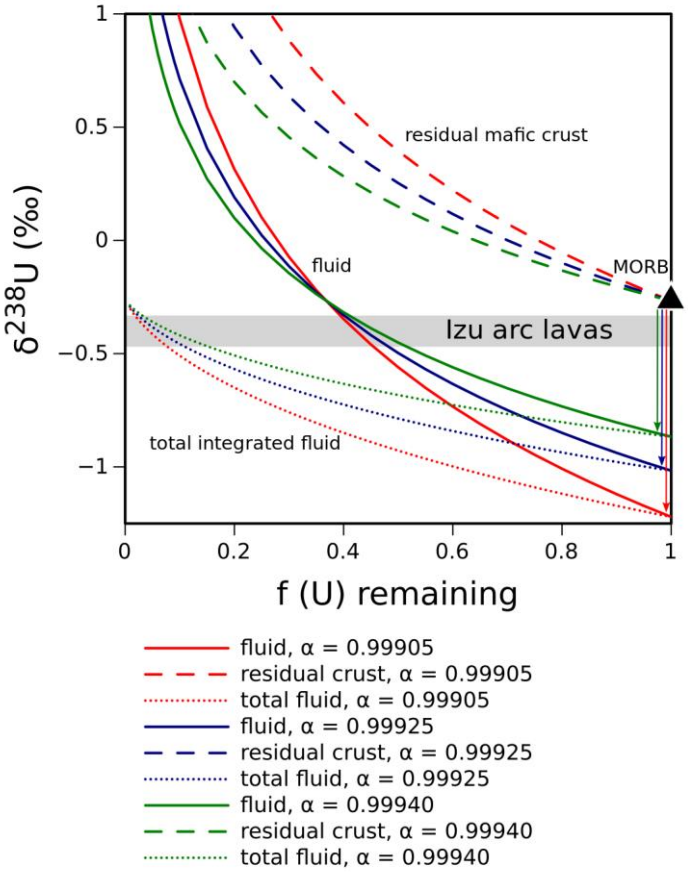
1
0.5
0
−0.5
−1
0
0.2
0.4
0.6
0.8
1
δ238U (‰)
f (U) remaining
residual mafic crust
fluid
MORB
Izu arc lavas
total integrated fluid
fluid, α = 0.99905
residual crust, α = 0.99905
total fluid, α = 0.99905
fluid, α = 0.99925
residual crust, α = 0.99925
total fluid, α = 0.99925
fluid, α = 0.99940
residual crust, α = 0.99940
total fluid, α = 0.99940

509

Table 1: Pb and U isotope ratios in Izu arc lavas. 2SE = 2σ standard error of individual analyses. 2SD = 2σ standard deviation of n separate sample dissolutions and isotope ratio analyses.

Sample	island	$^{206}Pb/^{204}Pb$	2SE	$^{207}Pb/^{204}Pb$	2SE	$^{208}Pb/^{204}Pb$	2SE	$\delta^{238}U$	2SE	$(^{234}U/^{238}U)$	2SE
1986A-1	Oshima	18.426	0.002	15.551	0.000	38.348	0.001	−0.424	0.027	1.0021	0.0018
S2-1	Oshima	18.427	0.001	15.552	0.001	38.352	0.002				
N4-1	Oshima	18.426	0.000	15.553	0.000	38.354	0.001	−0.449	0.022	1.0016	0.0009
1874 lava	Miyakejima	18.307	0.000	15.508	0.001	38.113	0.003				
1469	Miyakejima	18.310	0.001	15.510	0.001	38.120	0.001				
MJ-12-02	Miyakejima	18.306	0.001	15.505	0.001	38.102	0.005	−0.414	0.019	1.0019	0.0008
MJ-12-05	Miyakejima	18.306	0.001	15.502	0.001	38.086	0.003				
1983	Miyakejima	18.237	0.001	15.520	0.001	38.061	0.001	−0.381	0.021	1.0019	0.0009
3102807	Hachijojima	18.409	0.002	15.547	0.002	38.308	0.006				
3103009	Hachijojima	18.422	0.001	15.554	0.000	38.356	0.001	−0.476	0.017	1.0005	0.0008
3102804	Hachijojima	18.411	0.001	15.548	0.001	38.318	0.001				
03102812A	Hachijojima	18.413	0.001	15.548	0.001	38.318	0.003	−0.458	0.021	1.0002	0.0007
R69773/881 105-2	Aogashima	18.435	0.001	15.546	0.001	38.356	0.001	−0.392	0.021	1.0014	0.0010
T87071906	Aogashima	18.451	0.000	15.552	0.001	38.376	0.004	−0.415	0.033	1.0028	0.0022
TS-01-01	Torishima	18.440	0.001	15.556	0.001	38.321	0.005	−0.398	0.023	1.0031	0.0009
TS-08-11	Torishima	18.456	0.013	15.535	0.016	38.278	0.052				
TS-17-24	Torishima	18.380	0.002	15.562	0.002	38.288	0.007	−0.411	0.019	1.0034	0.0012
TS-22-37	Torishima	18.482	0.001	15.557	0.002	38.353	0.006				
NJ1	Niijima	18.308	0.002	15.544	0.003	38.249	0.009	−0.333	0.019	1.0033	0.0010

								−0.34			
NJ2	Niijima	18.292	0.003	15.540	0.004	38.243	0.013	8	0.018	1.0030	0.0009
				standards							
			2SD		2SD		2SD				
BCR-2 (n=3 for Pb, n =1								−0.28			
for U)		18.764	0.016	15.627	0.002	38.743	0.011	8	0.016	1.0027	0.0006
JB-2 (n=5)		18.343	0.008	15.562	0.006	38.276	0.023				

510

511

Table 2: Parameters used for U-Pb isotope models shown in Fig. 5.

	AOC	AOC melt	sediment	sediment melt	fluid source	fluid
Th (μg/g)	0.173 (1)	0.720 (4)	4.39 (5)	18.3 (4)	0.385 (8)	0.276 (11)
U (μg/g)	0.390 (1)	1.56 (4)	0.92 (5)	3.67 (4)	0.121 (8)	0.451 (11)
Pb (μg/g)	0.437 (1)	3.40 (4)	15.4 (5)	119 (4)	0.514 (8)	4.236 (12)
$\delta^{238}U$	-0.17 (2)	-0.17 (2)	-0.35 (6)	-0.35 (6)	-0.522 (9)	-0.522 (9)
$^{206}Pb/^{204}Pb$	19.137 (3)	19.137 (3)	18.589 (7)	18.589 (7)	18.052 (10)	18.052 (10)
$^{207}Pb/^{204}Pb$	15.533 (3)	15.533 (3)	15.587 (7)	15.587 (7)	15.480 (10)	15.480 (10)
$^{208}Pb/^{204}Pb$	37.896 (3)	37.896 (3)	38.558 (7)	38.558 (7)	37.887 (10)	37.887 (10)

(1) Site 801 AOC super composite, Kelley et al. (2005)

(2) Site 801 AOC super composite, Andersen et al. (2015)

(3) median of Indian MORB (https://www.earthchem.org/petdb)

(4) trace element concentrations calculated using 4 GPa, 900C partition coefficients from Kessel et al. (2005) with F = 0.1

(5) ODP Site 1149 average sediment, Plank et al. (2005)

(6) average sediment ODP Sites 801, 802 (volcaniclastics and pelagic clay), Andersen et al. (2015)

(7) ODP Site 1149 average sediment, Plank et al. (2007)

(8) average MORB (Jenner and O'Neill, 2012)

(9) from the trendline through the Mariana arc lavas (Fig. 2b) using Th/U as in (8)

(10) median of Indian MORB (PetDB)

(11) trace element concentrations calculated using the 4 GPa partition coefficients from Turner et al. (2003) with F = 0.1

(12) the Pb concentration was calculated as in (11) with the exception that the Pb fluid partition coefficient was calculated from the partition coefficient of U with a correction applied that takes the higher fraction of Pb lost

from the slab in the sub-arc region into account (Kelley et al., 2005)

512

513